SIMULATING AND MITIGATING IONOSPHERIC EFFECTS IN SYNTHETIC APERTURE RADAR

A. Philip Roth, Barton D. Huxtable, Kancham Chotoo, Susan D. Chotoo

User Systems, Incorporated

1. INTRODUCTION

The ionosphere is magnetized plasma that forms above the neutral atmosphere due to solar ionization of upper atmospheric constituents. It represents an obstacle to space based synthetic aperture radar (SAR) systems since it affects the radar signals traveling through it. Its impact can be split into two groups: uniform effects (those caused by a uniform and non-turbulent ionosphere) and non-uniform effects (those caused by irregularities in the ionosphere). In this paper, we present a method for simulating the uniform, non-turbulent effects such as dispersion, group delay, Faraday rotation, and phase shift. We also present quantitative examples of all these effects and discuss what this means for future space based SAR systems such as ALOS-2.

2. HOMOGENOUS SLAB IONOSPHERE SIMULATION

We assume a horizontally homogenous (vertical variations are allowed) and temporally invariant ionosphere. These spatial and temporal symmetries imply that the ionosphere's effect on SAR phase history data can be simply expressed in the Fourier domain by a multiplicative phase function $\Phi(k,\omega)$ of along-track wavenumber k and temporal frequency ω. Defining d(x,t) as the phase history data without the ionosphere, and $D(k,\omega)$ as that phase history data in Fourier coordinates, then: $D_{iono}(k,\omega) = \Phi(k,\omega)\, D(k,\omega)$. If this phase factor is known, it can easily be applied to SAR phase history data in order to simulate the ionosphere. In order to find this phase factor, we consider the propagation of an electromagnetic wave ($\exp(2\pi i(\omega t - kx))$ through a plasma. Starting from Maxwell's equations, a very general expression for the index of refraction for ordinary (+) and extraordinary (-) waves can be derived [1]:

$$n_{\pm}^2 = 1 - \frac{X}{1 - \frac{Y_T^2}{2(1-X)} \pm \sqrt{\frac{Y_T^4}{4(1-X)^2} + Y_L^2}}$$

with the following constants defined:

$$X = \frac{Ne^2}{(2\pi)^2 \varepsilon_0 m \omega^2} = \frac{\omega_p^2}{\omega^2} \qquad Y_L = \frac{\mu_0 He}{2\pi m \omega} \cos\varphi = \frac{\omega_L}{\omega} \qquad Y_T = \frac{\mu_0 He}{2\pi m \omega} \sin\varphi = \frac{\omega_T}{\omega}$$

In these equations, N is the electron density, H is the geomagnetic field density, e and m are the charge and mass of the electron, ε_0 and μ_0 are the electric and magnetic constants, and φ is the angle between the propagation and the magnetic field. The ordinary waves are right circular polarized waves propagating parallel to H or left circular propagating anti-parallel to H. Extraordinary waves are all others. For the frequencies of interest (ω_p ~ 12 MHz, ω_c ~ 1.4 MHz, and ω ~ 230 MHz to 40 GHz), the quasi-longitudinal approximation, defined as:

$$\frac{\sin^2\varphi}{2\cos\varphi} << \frac{\omega^2-\omega_p^2}{\omega_c\omega}$$

applies for most angles ($\varphi < 86^o$). Now, the index of refraction can be simplified to:

$$n_\pm - 1 = -\frac{1}{2}X\left(1 \mp Y_L\right) = -\frac{Ne^2}{(2\pi)^2\varepsilon_0 m\omega^2}\left(1 \mp \frac{\mu_0^2 eB\cos\varphi}{2\pi m\omega}\right)$$

At this point, the accumulated phase delay from the ionosphere can then be derived:

$$\Phi_\pm(\omega,\kappa) = \int \frac{2\pi\omega}{c}\left(n_\pm - 1\right)ds = -\frac{e^2\sec\theta_{inc}TEC}{2\pi\varepsilon_0 mc^2}\left(1 \mp \frac{Be\cos\varphi}{2\pi m\omega}\right)\left(\sqrt{\left(\frac{2\omega}{c}\right)^2 - \kappa^2}\right)^{-1}$$

where the integral is performed along the wave path through the ionosphere, θ_{inc} is the inclination angle, and TEC is the integrated total electron count of the ionosphere. TEC values increase with increasing altitudes to a peak value at around 250 to 400 km. Ninety-five percent of the electron content lies within 300 km of this peak. Since most space based SAR systems will orbit above this level, the value of TEC is effectively the same as the TEC taken directly from models based on GPS satellite signals [2]. This phase function provides a complete first-order scattering theory [3] description of the horizontally homogeneous ionosphere's effect on SAR data.

3. EXAMPLE RESULTS

We have taken the homogeneous slab ionosphere simulation and applied it to fully polarimetric data of the Washington, DC area from PALSAR. The original imagery was subject to ionospheric effects when it was collected, so those effects were first removed (Fig. 1). The images were then converted to circular polarization and put through the SAR image formation process in reverse to obtain the phase history data in the Fourier domain. The ionospheric phase delay was then easily applied at various levels of TEC, and phase history data was again put through normal image formation processing and converted back to linear polarization. Three ionospheric effects can then be directly measured from the resultant images: Faraday rotation, range shift, and image blurring.

3.1. Faraday Rotation

When travelling through the ionosphere, a linear polarized radio wave will split into two oppositely rotating circularly polarized waves travelling with slightly different velocities. When those waves exit the ionosphere and

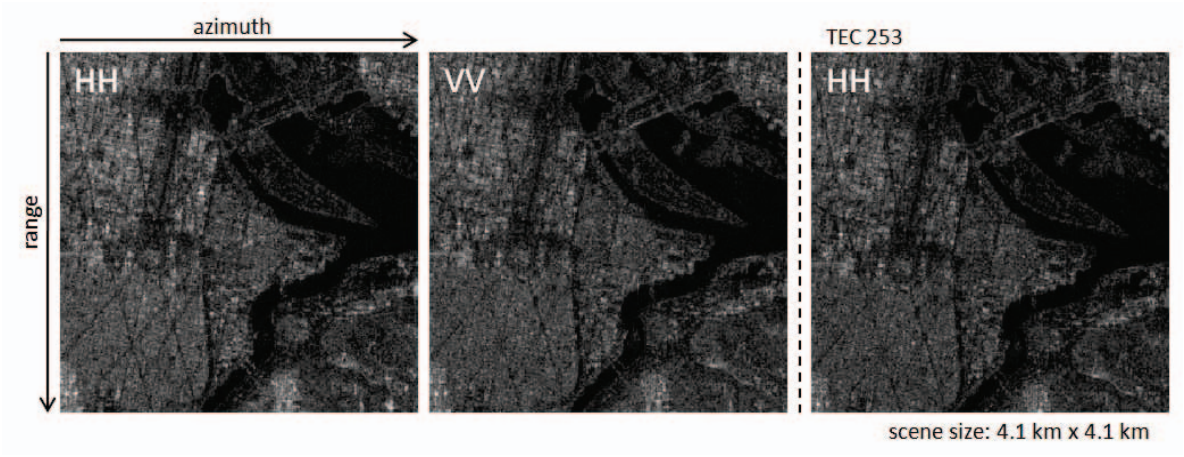

Fig. 1. PALSAR imagery of Washington, DC area corrected for ionospheric effects, HH channel (left) and VV channel (middle). The HH image is subjected to a 253 TEC simulated ionosphere (right). The Faraday rotation is 90^{o} at 253 TEC causing the HH image to be rotated into the VV. As a result, the simulated image more closely resembles the original VV channel image.

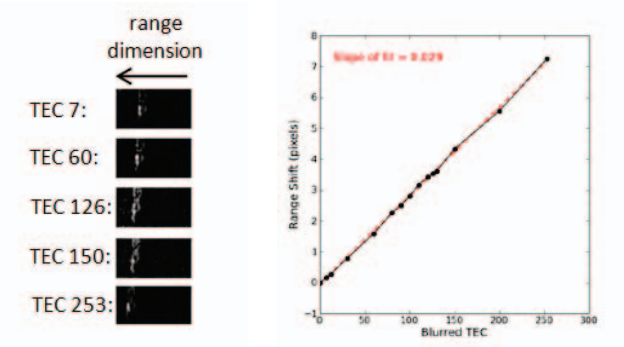

Fig. 2. A close up of a distinct object in images simulated with increasing levels of TEC (left). The movement toward far range is evident. The pixel position of this object as a function of simulated TEC, with fit (right).

recombine, those waves will have a slightly different linear polarization. This results in mixing of polarimetric channels, an increase in polarimetric cross talk, and reduced image contrast. The Faraday rotation can be calculated from the physical parameters of the scene [1]:

$$\Omega = \frac{\pi}{\lambda}\int (n_{+} - n_{-})ds = \frac{K}{\omega^2}\int NB\cos\varphi\sec\theta_{inc}\,dh = \frac{KB\cos\varphi\sec\theta_{inc}}{\omega^2}TEC$$

$$\text{with } K = \left(\frac{e^3}{8\pi^2\varepsilon_0 m^2 c}\right) = 2.365\times10^4\, A\cdot m^2\cdot kg^{-1}$$

Given fully polarimetric SAR data, the Faraday rotation present in the scene can be directly calculated with [4]:

$$\Omega = \frac{1}{4}\arg\left(Z_{12}Z_{21}^{*}\right), \text{ with } \begin{bmatrix} Z_{11} & Z_{12} \\ Z_{21} & Z_{22} \end{bmatrix} = \begin{bmatrix} 1 & i \\ i & 1 \end{bmatrix}\cdot\begin{bmatrix} M_{hh} & M_{vh} \\ M_{hv} & M_{vv} \end{bmatrix}\cdot\begin{bmatrix} 1 & i \\ i & 1 \end{bmatrix}$$

In the PALSAR simulation, at each level of simulated TEC, the Faraday rotation was measured from the resultant images and compared to the physically calculated value, and the agreement was found to be very good.

3.2. Range Shift

As the simulated TEC is increased, features in the scene appear at farther and farther range. This range shift can be calculated analytically:

$$\Delta r = c\tau_{\pm} = \frac{c}{2\pi}\frac{\delta\Phi_{\pm}}{\delta\omega}\Big|_{\substack{\omega=\omega_0 \\ \kappa=0}} = \frac{e^2 \sec\theta_{inc} TEC}{8\pi^2\varepsilon_0 m\omega_0^3}\left(\omega_0 \mp \frac{Be\cos\varphi}{\pi m}\right) = 0.27\frac{m}{TEC}$$

This can then be compared to the range shift seen in the simulation itself by picking out one bright feature in the scene, and following its location through increasing levels of simulated TEC. The results are shown in Fig. 2.

The slope of the fit is multiplied by the pixel spacing of 9.3 m to get 0.27 m/TEC, which agrees with the analytically calculated number.

3.2. Image Blurring

As can be seen in Fig. 1, there is very little, if any, blurring in the simulated images for the polarimetric mode even as the TEC level is increased to unphysical levels. This can be confirmed analytically with:

$$\frac{\beta^2}{4\pi}\frac{\delta^2\Phi_{\pm}}{\delta\omega^2}\Big|_{\substack{\omega=\omega_0 \\ \kappa=0}} = \frac{e^2\beta^2 \sec\theta_{inc} TEC}{8\pi^2\varepsilon_0 mc\omega_0^4}\left(\omega_0 \mp \frac{3Be\cos\varphi}{2\pi m}\right) = 1.42\times10^{-4}\frac{cycles}{TEC}$$

Generally, every cycle of phase shift error adds another IPR width to the achievable theoretical resolution. Due to PALSAR's narrow bandwidth, this blurring is imperceptible at expected TEC levels.

4. DISCUSSION

The homogenous slab ionosphere simulation can be used to predict the effects that the ionosphere will have on future space based SAR systems. For example, published system parameters for ALOS-2 [5] imply a range shift of 0.26 m/TEC and image blurring at still imperceptible 4.65 x 10^{-3} IPR widths per unit of TEC even at the highest bandwidths. The ionospheric effects on applications such as InSAR can also be examined.

[1] Z. Xu, J. Wu, and Z. Wu, "A Survey of Ionospheric Effects on Space-Based Radar," *Waves in Random Media*, Institute of Physics Publishing, Bristol UK, **14** pp. S189-S273, 17 March 2004.

[2] P.A. Wright, S. Quegan, N.S. Wheadon, and C.D. Hall, "Faraday Rotation Effects on L-band Spaceborne SAR Data," *Trans. On Geoscience and Remote Sensing*, IEEE, New York NY, **41** 12 pp. 2735-2744, 2003.

[3] A. Ishimaru, *Wave Propagation and Scattering in Random Media*, IEEE Press, Piscataway NJ, pp. 338-366, 1997.

[4] S.H. Bickel and R.H.T. Bates, "Effects of Magneto-ionic Propagation on the Polarization Scattering Matrix," *Proc. IRE*, IEEE, New York NY, **53** pp. 1089-1091, 1965.

[5] Y. Kankaku, Y. Osawa, S. Suzuki, T. Watanabe, "The Overview of the L-band SAR Onboard ALOS-2," *Proc. PIERS*, The Electromagnetics Academy, Cambridge MA, pp. 735-738, August 18-21 2009.